Hybrid Beamforming With Discrete Phase Shifts for RIS-Assisted Multiuser SWIPT System

Zhen Chen, *Member, IEEE*, Jie Tang, *Senior Member, IEEE*, Nan Zhao, *Senior Member, IEEE*, Mingqian Liu, *Member, IEEE*, and Daniel Ka Chun So, *Senior Member, IEEE*

Abstract—Reconfigurable Intelligent Surfaces (RIS) provides an emerging affordable solution by leveraging massive low-cost reconfigurable reflective array elements. In this letter, by utilizing low-cost passive reflecting elements, a joint hybrid beamforming with discrete phase shifts design is studied in RIS-assisted multiuser simultaneous wireless information and power transfer (SWIPT) systems. However, the formulated sum rate maximization problem is nonconvex and very challenging to solve. To overcome this difficulty, we decouple the original maximization problem into the digital-, phase shifts and analog subproblem. Specifically, for the nonconvexity of the digital sub-problem, we perform the first order Taylor series expansion on the objective function, and then an iterative strategy is developed to tackle the difficulty of the maximum transmit power constraint imposed by discrete optimization variables. Subsequently, an effective convex optimization technique was employed to optimize reflecting elements of RIS. Finally, the greedy selection method based on minimum mean squared error (MMSE) scheme is proposed to solve the analog subproblem. Numerical simulations are conducted to demonstrate the performance advantages of the proposed scheme.

Index Terms—Hybrid beamforming, reconfigurable intelligent surfaces, SWIPT, multiuser MIMO.

I. INTRODUCTION

THE INCREASING demand for high data rate and ubiquitous services has led to a large energy consumption the fifth-generation (5G) and beyond era. To cope with these challenges, the environmentally-friendly energy harvesting (EH) technology is proposed to harvest renewable energy from the environment to extend the working life of the equipment. However, due to the variability of weather and the influence of geographical location, natural energy sources are often unstable and unpredictable. Recently, great interests have been drawn in simultaneous wireless information and power transfer (SWIPT), proposed by Varshney [1], in which energy and information are transferred at the same time. To enable practical techniques to convey information and power, SWIPT was widely studied in various communication networks [2], [3]. Specifically, these studies were mainly focused on the expected capacity maximization problem under the harvested power constraint or sum-harvested power maximization with quality-of-service (QoS) constraint. However, it requires a significant amount of radio frequency (RF) chains that may result in high power consumption in 5G communication or Internet of Things (IoT) networks; thereby it is disadvantage to the practical implementation. Interestingly, the new research paradigm of reconfigurable intelligent surfaces (RIS)-assisted SWIPT communication has been extensively studied recently [4], [5]. RIS can enhance the coverage of network and improve spectral and energy efficiencies (EE), especially in specificities of typical urban scenarios suffering from severe blockage [5]. Compared with the conventional active beamforming/relaying technologies, RIS can adjust the incident signals to achieve a high level of energy focusing at the receiver without signal amplification and regeneration. Since low hardware cost of the reflecting elements, the RIS can be deployed easily to improve the spectral efficiency (SE) of multiuser multiple input multiple output (MIMO) system, while SWIPT can provide more incentives for user cooperation. Therefore, it is natural to consider the combination of RIS and SWIPT in cooperative networks, which greatly increases the service range and improves the wireless power transfer (WPT) efficiency for a cluster of energy harvesting receivers (EHR) (e.g., IoT sensors) located in an energy charging.

To reap this benefit, there have been many reports regarding the SE maximization problems in RIS-assisted SWIPT networks [4], [5], [6], [7]. In [6], the specific absorption rate (SAR)-constrained multiuser transmit beamforming optimization with QoS requirements are investigated to achieve a better performance-complexity tradeoff. In [4], the max-min signal-to-interference-plus-noise ratio (SINR) optimization of the RIS-assisted SWIPT system is investigated, in which transmits beamforming and the passive RIS with discrete phase shifts are jointly optimized. In [8], authors develop holographic MIMO surfaces for diverse wireless communication applications. Subsequently, authors investigated channel estimation approach for RIS-based downlink

Zhen Chen is with the School of Electronic and Information Engineering, Shenzhen University, Shenzhen 518060, China, and also with the State Key Laboratory of Integrated Service Networks, Xidian University, Xi'an 210096, China (e-mail: chenz.scut@gmail.com).

Jie Tang is with the School of Electronic and Information Engineering, South China University of Technology, Guangzhou 510641, China (e-mail: eejtang@scut.edu.cn).

Nan Zhao is with the School of Information and Communication Engineering, Dalian University of Technology, Dalian 116024, China (e-mail: zhaonan@dlut.edu.cn).

Mingqian Liu is with the State Key Laboratory of Integrated Service Networks, Xidian University, Xi'an 210096, China (e-mail: mqliu@mail.xidian.edu.cn).

Daniel Ka Chun So is with the School of Electrical and Electronic Engineering, University of Manchester, M13 9PL Manchester, U.K. (e-mail: d.so@manchester.ac.uk).

Digital Object Identifier 10.1109/LWC.2022.3218332
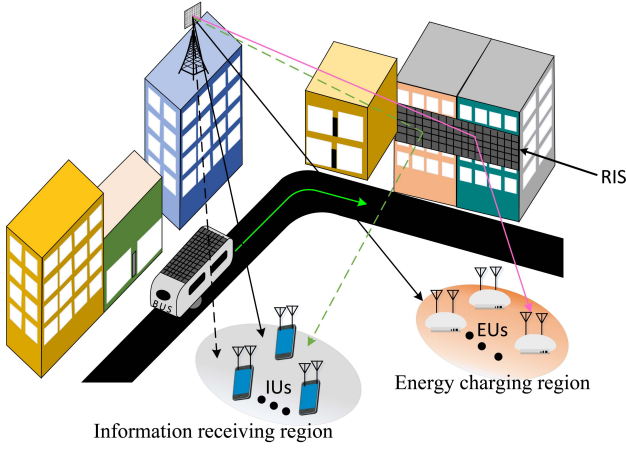
multi-user MISO system [9] and so on. By integrating RIS into SWIPT, the formulated optimization problem can effectively solve the performance fairness issue to a certain extent. However, since the base station (BS) transmit beamforming vectors and the reflecting elements of RIS are strongly coupled in the constrained objective function, such combinatorial optimization problem is generally nonconvex and computationally intractable, to which the derivation of the optimal solution is still an open issue.

In this letter, joint digital-, phase shifts and analog design is investigated for RIS-assisted multiuser SWIPT system, where the BS serves the information users (IUs) and energy users (EUs) simultaneously. The considered maximization problem involves the harvested energy and transmit power constraint, which is non-convex and hard to solve directly. To tackle this intractable problem, we decouple the maximization problem into the digital domain, phase shift and analog domain processing stage, and solve them sequentially. In the digital domain processing stage, we derive linear approximation of the objection function with first order Taylor series expansion, and then an iterative algorithm is utilized to find the sub-optimal digital precoder/combiner. After finishing the digital precoder/combiner design, the effective convex optimization technique with quantized phase scheme is employed to optimize reflecting elements of RIS. In the analog processing stage, the analog precoding matrix is divided into a number of vectors, and then the greedy selection algorithm is proposed for analog precoder/combiner design. Finally, the effectiveness of the proposed scheme is verified by simulations.

II. PROBLEM FORMULATION

As depicted in Fig. 1, the RIS-assisted multiuser SWIPT system consists of one BS with N_t antennas employing M_t RF chains, K information users with N_r antennas using M_r RF chains, $\mathcal{M}$ energy harvesting users with N_r antennas. Moreover, the BS transmit N_s data streams to the IUs, and each IU receive d data streams, thus the transmitted streams satisfies $Kd = N_s \leq M_t \leq N_t$ and $d \leq M_r \leq N_r$. Moreover, the N_s data streams are processed by the $N_t \times M_t$ digital beamformer $\boldsymbol{B} = [\boldsymbol{B}_1, \ldots, \boldsymbol{B}_K]$, $\boldsymbol{B}_k \in \mathbb{C}^{N_t \times d}$, and then connected by an $M_t \times N_t$ analog beamformer $\boldsymbol{F}$. The RIS $\boldsymbol{\Omega} \in \mathbb{C}^{M_t \times M_t}$ is deployed on both the users and the BS. On the other hand, the k-th IU processed the received signals by an $N_r \times M_r$ analog combiner $\boldsymbol{W}_k$, then followed by

an $d \times N_r$ baseband combiner $\boldsymbol{M}_k$. Thus, the received signal is mathematically formulated as

$$\boldsymbol{y}_k = \boldsymbol{M}_k \boldsymbol{W}_k \boldsymbol{H}_k \boldsymbol{F} \sum_{k=1}^{K} \boldsymbol{B}_k \boldsymbol{s}_k + \boldsymbol{M}_k \boldsymbol{W}_k \boldsymbol{n}_k, \forall k, \quad (1)$$

where $\boldsymbol{s} = [\boldsymbol{s}_1^T, \ldots, \boldsymbol{s}_K^T]^T$ denotes the transmitted signal, and it is assumed that $\mathbb{E}[\boldsymbol{s}_k \boldsymbol{s}_k^*] = \boldsymbol{I}_{N_s}, \forall i \neq k$, the vector $\boldsymbol{n}_k \in \mathbb{C}^{d \times 1}$ denotes the noise vector.

A. RIS-Assisted Channel Modeling

According to the (1), the extended Saleh-Valenzuela geometric model is used to model the RIS-assisted channel. By specifying the prorogation environment, the BS-RIS channel $\boldsymbol{H}_{BI}$ is defined as

$$\boldsymbol{H}_{BI} = \sqrt{\frac{N_t N_{RIS}}{N_c N_p}} \sum_{i=1}^{N_c} \sum_{l=1}^{N_p} \alpha_{i,l} \boldsymbol{a}_{RIS}(\phi_{i,l}^{RIS}, \theta_{i,l}^{RIS}) \boldsymbol{a}_t^*(\phi_{i,l}^t, \theta_{i,l}^t), (2)$$

where $\alpha_{i,l} \in \mathcal{CN}(0, \sigma_{i,l}^2)$ denotes the complex gain of the l-th path in the i-th scattering cluster. Moreover, $\mathbf{a}_{RIS}(\phi_{i,l}^{RIS}, \theta_{i,l}^{RIS})$ and $\mathbf{a}_t(\phi_{i,l}^t, \theta_{i,l}^t)$ denote the receive and transmit array response vectors, where $\phi_{i,l}^{RIS}$ and $\theta_{i,l}^{RIS}$ represent the angles of departure/arrival (AoDs/AoAs), respectively.

Similarly, the RIS-IU channel $\boldsymbol{H}_{IU}$ is given by

$$\boldsymbol{H}_{IU} = \sqrt{\frac{N_r N_{RIS}}{N_c N_p}} \sum_{i=1}^{N_c} \sum_{l=1}^{N_p} \beta_{i,l} \boldsymbol{a}_r(\phi_{i,l}^r, \theta_{i,l}^r) \boldsymbol{a}_{RIS}^*(\phi_{i,l}^{RIS}, \theta_{i,l}^{RIS}), (3)$$

where $\beta_{i,l}, \mathbf{a}_r(\phi_{i,l}^r, \theta_{i,l}^r), \mathbf{a}_{RIS}^*(\phi_{i,l}^{RIS}, \theta_{i,l}^{RIS})$ are the l th propagation path gain, and array response vectors, respectively. The BS-RIS-IU$_k$ channel based on (2) and (3) is defined as

$$\boldsymbol{H}_k = \boldsymbol{H}_{IU_k} \boldsymbol{\Omega} \boldsymbol{H}_{BI}, \quad (4)$$

where $\boldsymbol{\Omega} \in \mathbb{C}^{M_t \times M_t}$ is the diagonal phase control matrix of RIS, denoted by $[\boldsymbol{\Omega}]_{k,k} = e^{j\omega_k}$. Thus, the BS-RIS-EU$_k$ channel $\boldsymbol{G}_m$ is given by

$$\boldsymbol{G}_m = \boldsymbol{H}_{IE,m} \boldsymbol{\Omega} \boldsymbol{H}_{BI}, \quad (5)$$

where $\boldsymbol{H}_{IE,m} \in \mathbb{C}^{N_r \times M_t}$ denotes complex channel matrix from the RIS to the m-th EU. Therefore, the SE of k-th IU can be written as

$$R_k = \log_2 \det(\boldsymbol{I} + \boldsymbol{T}_k^{-1} \boldsymbol{M}_k \boldsymbol{W}_k \boldsymbol{H}_k \boldsymbol{F} \boldsymbol{B}_k \boldsymbol{B}_k^* \boldsymbol{F}^* \boldsymbol{H}_k^* \boldsymbol{W}_k^* \boldsymbol{M}_k^*), \quad (6)$$

where $\boldsymbol{T}_k = \sum_{i \neq k}^{K} \boldsymbol{M}_k \boldsymbol{W}_k \boldsymbol{H}_k \boldsymbol{F} \boldsymbol{B}_i \boldsymbol{B}_i^* \boldsymbol{F}^* \boldsymbol{H}_k^* \boldsymbol{M}_k^* \boldsymbol{W}_k^* + \boldsymbol{M}_k \boldsymbol{W}_k \boldsymbol{W}_k^* \boldsymbol{M}_k^* \sigma_n^2$ denotes the covariance of the interference plus noise at k-th IU. For the EUs, the total EH of the m-th EU can be written as

$$E_m = \eta_m \sum_{k=1}^{K} \text{tr}(\boldsymbol{G}_m \boldsymbol{F} \boldsymbol{B}_k \boldsymbol{B}_k^* \boldsymbol{F}^* \boldsymbol{G}_m^*), \forall m \quad (7)$$

where η_m is the energy conversion rate of the m-th EU.

Our aim is to design the digital beamformer $\boldsymbol{B}$, analog beamformer $\boldsymbol{F}$, phase shifts $\boldsymbol{\Omega}$, the analog combiner $\boldsymbol{W}$ and the digital combiner $\boldsymbol{M}$ by maximizing the SE of system, subject to the minimum EH requirement and transmit power constraint.

Fig. 1. The RIS-assisted multiuser SWIPT system.

Therefore, the proposed hybrid beamforming design problem can be expressed mathematically as

$$(P_0) \quad \max_{\boldsymbol{B},\boldsymbol{F},\boldsymbol{\Omega},\{\boldsymbol{W}_k,\boldsymbol{M}_k\}_{k=1}^K} \sum_{k=1}^K R_k \tag{8a}$$

$$s.t. \quad E_m \geq \bar{E}_m, \; \forall m \tag{8b}$$

$$\|\boldsymbol{F}\boldsymbol{B}\|_F^2 \leq P \tag{8c}$$

$$|\boldsymbol{F}(i,j)|^2 = 1, \forall i,j \tag{8d}$$

$$|\boldsymbol{W}_k(i,j)|^2 = 1, \forall i,j,k \tag{8e}$$

where $\bar{E}_m$ is the minimum EH required by the m-th EU. The corresponding optimization problem is a non-convex, due to the constant magnitude of precoder/combiner matrix and the transmit power constrains.

III. Hybrid Beamforming With Discrete Phase Shift Design

For the optimization problem mentioned above, multiple variables need to be optimized jointly, so it is intractable to obtain the optimal solution. Based on this, we decouple the maximization problem into a series of subproblem. The analog precoder/combiner is achieved by approximating the objective function. Then, discrete phase shift of RIS is designed by exploiting the quantized phase scheme. Finally, the digital precoder/combiner of all the IUs are designed based on an MMSE scheme. In the following section, we will simplify the optimization problem to seek a near-optimal solution.

A. Analog Domain Design

The analog precoder and combiner is optimized by maximizing the mutual information over the channel, the problem (8) with respect to $\boldsymbol{F}, \{\boldsymbol{W}_k\}_{k=1}^K$ are given by

$$\max_{\boldsymbol{F},\{\boldsymbol{W}_k\}_{k=1}^K} \sum_{k=1}^K \log_2 \; \det(\boldsymbol{I}_{M_r} + \boldsymbol{W}_k \boldsymbol{H}_k \boldsymbol{F}\boldsymbol{F}^* \boldsymbol{H}_k^* \boldsymbol{W}_k^*) \tag{9a}$$

$$s.t. \quad (8d),(8e) \tag{9b}$$

Since the structures of the analog precoder/combiner are similar, the design of $\boldsymbol{F}$ and $\{\boldsymbol{W}_k\}_{k=1}^K$ can be separated to reduce the complexity of the problem. Firstly, the analog precoder $\boldsymbol{F}$ is designed by assuming $\boldsymbol{W}_k \boldsymbol{W}_k^* = \boldsymbol{I}_{N_r}, \forall k$. Then, we optimize $\{\boldsymbol{W}_k, \forall k\}$ with $\hat{\boldsymbol{H}} = \boldsymbol{H}\boldsymbol{F}$. Therefore, the objective function of the optimization problem for the analog precoder and combiner can be written as

$$\max_{\boldsymbol{F}} \sum_{k=1}^K \log_2 \det(\boldsymbol{I}_{N_r} + \boldsymbol{H}_k \boldsymbol{F}\boldsymbol{F}^* \boldsymbol{H}_k^*), \tag{10}$$

$$\max_{\{\boldsymbol{W}_k\}_{k=1}^K} \sum_{k=1}^K \log_2 \det\left(\boldsymbol{I}_{N_r} + \boldsymbol{W}_k \hat{\boldsymbol{H}}_k \hat{\boldsymbol{H}}_k^* \boldsymbol{W}_k^*\right). \tag{11}$$

Considering the magnitude of precoder/combiner constraint, it is intractable to solve the above problem directly. For the fairness of users, we divide the analog precoding matrix into several sub-matrices. We define $\boldsymbol{F} = [\boldsymbol{F}_1, \boldsymbol{F}_2, \ldots, \boldsymbol{F}_K]$, where each analog precoder $\boldsymbol{F}_k$ serves the k-th IU. Thus, the problem (10) is reformulated as

---

Algorithm 1 Greedy Selection Algorithm

Require: M_t, $\boldsymbol{H}_k$ and $\boldsymbol{A}_t^k$, $1 \leq k \leq K$
1: **Initialization**: $\boldsymbol{F}_k = \emptyset$, $\boldsymbol{T} = \boldsymbol{I}_{N_r}$ $\boldsymbol{F}_k$, $1 \leq k \leq K$
2: **for** $1 < k \leq K$ **do**
3:      **for** $i = 1$ to M_t **do**
4:          Select a column of $\boldsymbol{A}_t^k$, named as $\boldsymbol{f}_n$ to maximize the problem (16)
5:          Update $\boldsymbol{F}_k = [\boldsymbol{F}_k, \boldsymbol{f}_n]$, $\boldsymbol{A}_t^k = \boldsymbol{A}_t^k - \{\boldsymbol{f}_n\}$
6:          Update $\boldsymbol{T} = \boldsymbol{T} + \boldsymbol{H}_k \boldsymbol{f}_n \boldsymbol{f}_n^* \boldsymbol{H}_k^*$
7:      **end for**
8: **end for**

$$\max_{\boldsymbol{F}} \quad \sum_{k=1}^K \log_2 \det\left(\boldsymbol{I}_{N_r} + \sum_{j=1}^K \boldsymbol{H}_k \boldsymbol{F}_j \boldsymbol{F}_j^* \boldsymbol{H}_k^*\right) \tag{12a}$$

$$s.t. \quad \boldsymbol{F}_j \in \left\{ \boldsymbol{a}_t^j(\phi_{i,\ell}^t, \theta_{i,\ell}^t), \forall i, \ell \right\}, \tag{12b}$$

where $\mathbf{a}_t^j$ denotes the array response vectors corresponding to the AODs from the BS to the j-th users.

Inspired by [10], when the AODs and AOAs are drawn independently from a continuous distribution, we have

$$\boldsymbol{F}_j^* \boldsymbol{F}_k = \boldsymbol{0}, \quad \forall j \neq k. \tag{13}$$

Therefore, the problem (12) can be further simplified as K sub-problems, which can be written as follow

$$\max_{\boldsymbol{F}_k} \; \log_2 \det(\boldsymbol{I}_{N_r} + \boldsymbol{H}_k \boldsymbol{F}_k \boldsymbol{F}_k^* \boldsymbol{H}_k^*) \tag{14a}$$

$$s.t. \quad \boldsymbol{F}_k \in \left\{ \mathbf{a}_t^k(\phi_{i,\ell}^t, \theta_{i,\ell}^t), \forall i, \ell \right\}, \; k = 1, \ldots, K. \tag{14b}$$

According to the problem (14), we decompose the analog precoder $\boldsymbol{F}_k$ as $\boldsymbol{F}_k = [\boldsymbol{F}_{N-1}, \boldsymbol{f}_n]$, where $\boldsymbol{f}_n$ is the n-th column of $\boldsymbol{F}_k$, and $\boldsymbol{F}_{k,N-1}$ is the first $N-1$ columns of $\boldsymbol{F}_k$. Thus, the objective function of the problem (14) is given by

$$C_n = \log_2 \det\left(\boldsymbol{I}_{N_r} + \boldsymbol{H}_k \boldsymbol{F}_{N-1} \boldsymbol{F}_{N-1}^* \boldsymbol{H}_k^* + \boldsymbol{H}_k \boldsymbol{f}_n \boldsymbol{f}_n^* \boldsymbol{H}_k^*\right)$$
$$\overset{(a)}{=} \log_2 \det(\boldsymbol{T}_{N-1}) + \log_2\left(1 + \boldsymbol{f}_n^* \boldsymbol{H}_k^* \boldsymbol{T}_{N-1}^{-1} \boldsymbol{H}_k \boldsymbol{f}_n\right), \tag{15}$$

where (a) is from $\boldsymbol{T}_{N-1} = \boldsymbol{I}_{N_r} + \boldsymbol{H}_k \boldsymbol{F}_{N-1} \boldsymbol{F}_{N-1}^* \boldsymbol{H}_k^*$. For the case $n = 0$, we define that $\boldsymbol{T}_0 = \boldsymbol{I}_{N_r}$. It is observed that the second equation is not negative, which implies that C_n is an increasing function with respect to n. Therefore, we can search the whole array response matrix $\boldsymbol{A}_t^k$ and choose the best column to solve the above problem by maximizing the objective function as follows

$$\max_{\boldsymbol{f}_n} \log_2 \det(\boldsymbol{T}_{N-1}) + \log_2\left(1 + \boldsymbol{f}_n^* \boldsymbol{H}_k^* \boldsymbol{T}_{N-1}^{-1} \boldsymbol{H}_k \boldsymbol{f}_n\right). \tag{16}$$

Similarly, this scheme also is applied to design $\boldsymbol{W}_k$ by substituting $\hat{\boldsymbol{H}}_k$ and $\boldsymbol{A}_r^k$, respectively. In summary, the pseudo-code is given in Algorithm 1. Note that [] and {} denotes the set union of two sequences and set, respectively.

B. RIS's Phase Shift Design

It is not difficult to find that for given $\boldsymbol{\Omega}$, the capacity of k-th IU can be reformulated as

$$\max_{\boldsymbol{\Omega}_k} \; \log_2 \det\left(\boldsymbol{I}_{N_r} + \tilde{\boldsymbol{T}}^{-1} \boldsymbol{A}_m \boldsymbol{\Omega}_k \tilde{\boldsymbol{U}}_k \boldsymbol{\Omega}_k^* \boldsymbol{A}_m^*\right) \tag{17a}$$

$$s.t. \quad E_m \geq \bar{E}_m, \; \forall m \tag{17b}$$

Algorithm 2 Low Complex Hybrid Precoder Design

Require: $\tilde{H}_k$, $1 \leq k \leq K$, B_k, $1 \leq k \leq K$
1: Initialization: $Q_k = 0, \forall i$
2: **repeat**
3:      Update the optimal $Q_k, \forall k$, by solving the problem (22)
4:      Update $\bar{Q}_k = Q_k, \forall i$
5: **until** convergence
6: Calculate the B_k by decomposing Q_k with SVD.

---

where $\tilde{U}_k = H_{BI} F B_k B_k^* F^* H_{BI}^*$, $A_m = M_k W_k H_{IE,m}$, and $\tilde{T} = \sum_{i \neq k} A_m \Omega_k \tilde{U}_i^* \Omega_k^* A_m^* + M_k W_k W_k^* M_k^* \sigma_n^2$ denotes the covariance of the interference plus noise at k-th IU. Note that (17) is convex on optimization variable Ω, which can be solved by convex program.

It is worth noting that increasing RIS elements to improve system performance is a great energy-saving scheme. However, a large number of RIS elements result in a great increase in hardware requirements. For this purpose, we quantify the phase of the RIS element to further reduce the hardware complexity. Let $\theta_{i,j} \triangleq \angle\Omega(i,j)$, the quantized phase $\bar{\theta}_{i,j}$ can be derived by following calculation

$$\bar{\theta}_{i,j} = \text{round}\left(\frac{\theta_{i,j}}{\delta}\right) \times \delta, \tag{18}$$

where $\delta = \frac{2\pi}{2^B}$ denotes the resolution of phase shift, and B denotes the quantization bits.

C. Digital Domain Design

After the analog precoder F and combiners $\{W_k, \forall k\}$ are optimized, the digital precoder and combiners further are determined to maximize the SE of the problem (6). Therefore, the capacity of k-th IU is reformulated as

$$R_k = \log_2 \det\left(I_{N_r} + T^{-1} M_k \tilde{H}_k B_k B_k^* \tilde{H}_k^* M_k^*\right), \tag{19}$$

where $\tilde{H}_k = W_k H_k F$ denotes the equivalent channel.

To decouple the transceiver digital matrices, we focus on the design of the digital precoder B to maximize the mutual information achieved by training sequences or pilot signal over the equivalent channel, which can be written as

$$\max_{Q_k} \sum_{i=1}^{K} R_i \tag{20a}$$

$$s.t. \quad R_i = \log_2 \frac{\det\left(I + \sum_{k=1}^{K} \tilde{H}_i Q_k \tilde{H}_i^*\right)}{\det\left(I + \sum_{k=1,k \neq i}^{K} \tilde{H}_i Q_k \tilde{H}_i^*\right)}, \tag{20b}$$

where $Q_k = B_k B_k^*$. Obviously, the optimization problem (20) is non-concave because of the inter-user interference of the objection function R_k, which is difficult to be solved. Motivated by [11], we derive a linear approximation of the non-concave objection function to make it concave. The method aims to transform the function (20) into convex function by exploiting first order Taylor expansion. Thus, we can obtain the upper bound of $\log \det(I + X)$ as

$$\log \det(I + X) \leq \log \det(I + X_0)$$
$$+ \text{tr}\left((I + X_0)^{-1}(I - X_0)\right). \tag{21}$$

Therefore, the mutual information of i-th IU can be lower bounded at point $\sum_{k=1,k \neq i} \bar{Q}_k$ as

$$R_i \geq \log \det\left(I + \sum_{k=1}^{K} \tilde{H}_i Q_k \tilde{H}_i^*\right) - \sum_{k=1,k \neq i}^{K} \text{tr}(Y_i^{-1} \tilde{H}_i Q_k \tilde{H}_i^*)$$
$$- \log \det Y_i + \sum_{k=1,k \neq i}^{K} \text{tr}\left(Y_i^{-1} \tilde{H}_i \bar{Q}_k \tilde{H}_i^*\right) \triangleq \tilde{R}_i,$$

where $Y_i = I + \sum_{k=1,k \neq i} H_i \bar{Q}_k H_i^*$. Therefore, the maximization problem can be reformulated as

$$\max_{Q_k, \forall k} \sum_{1 \leq k \leq K} R_k \tag{22a}$$

$$s.t. \quad \sum_{k=1}^{K} \text{tr}(F Q_k F^*) \leq P \tag{22b}$$

$$E_m \geq \bar{E}_m, \forall m \tag{22c}$$

$$Q_i \succeq 0, \forall k. \tag{22d}$$

The above optimization problem can be solved using the convex optimization numerical techniques, such as the interior-point method [12]. By utilizing the singular value decomposition of Q_k, the precoder B_k of the k-th receiver can be calculated. In summary, the pseudo-code for the digital precoding algorithm is given in Algorithm 2.

After obtaining the hybrid precoder and analog combiner, the received signal is given by

$$y_k = M_k \tilde{H}_k B_k s_k + M_k \tilde{H}_k \sum_{i=1,i \neq k}^{K} B_i s_i + M_k W_k n_k. \tag{23}$$

We seek to design digital combiners M_k by minimizing the mean-squared-error (MSE). Thus, the solution of the digital combiner design is given by

$$M_k = \mathbb{E}[s_k y_k^*]\mathbb{E}\left[y_k y_k^H\right]^{-1}$$
$$= B_k^* \tilde{H}_k^*(\tilde{H}_k B B^* \tilde{H}_k^* + \sigma^2 W_k W_k^*)^{-1}, \forall k. \tag{24}$$

It follows that the digital-, phase shift and analog domain precoder can be optimized by the alternate optimization. Based on (P_0), the overall complexity of the above algorithm can be shown to be $\mathcal{O}(I(KN_t d^2 + N_t^3(K + M_t^2 N_t d) + N_r^2 M_r))$, where I denotes the iteration numbers required for convergence. In the following section, the simulations will be provided to verify the performance of proposed scheme.

IV. NUMERICAL SIMULATION

Numerical simulations are provided to evaluate the effectiveness of the proposed algorithm. The number of scattering cluster is $N_c = 8$ with $N_p = 10$ propagation paths, and the variance of path gain of each cluster is $\sigma_{i,l}^2 = 0.1, \forall i, l$. The AoDs and AoAs follow the Laplacian distribution with uniformly distributed mean angles over $[-\frac{\pi}{2}, \frac{\pi}{2}]$ and $[-\frac{\pi}{6}, \frac{\pi}{6}]$, respectively, and an angular spread of 6 degrees. All results are based on the basic principles of Monte Carlo simulation, and simulation results can be averaged over 5000 times. The BS is equipped with $N_t = 64$ antennas to serve $K = 4$ IUs and $Q = 4$ EUs with $N_r = 16$ antennas.

(a) SE against SNR levels with different beam-
forming methods.

(b) Transmit sum-power against EH threshold for
different number of RIS elements.

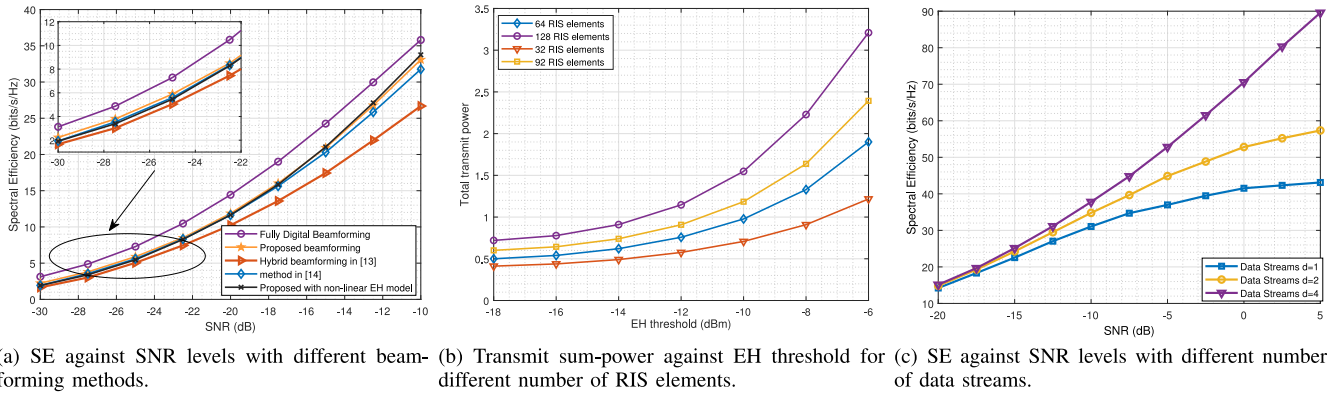(c) SE against SNR levels with different number
of data streams.

Fig. 2.   (a) SE against SNR levels with different beamforming methods. (b) Transmit sum-power against EH threshold for different number of RIS elements.
(c) SE against SNR levels with different number of data streams.

Firstly, we compare the performance of four different beam-forming methods: (1) Full digital beamforming; (2) hybrid beamforming with beamspace MIMO proposed in [13], (3) the scheme proposed in [14] and the proposed scheme with non-linear EH model. According to the non-linear EH model proposed by [15], we set parameters $c = 2.463$, $d = 1.635$ and $v = 0.826$. Fig. 2(a) illustrates the SE as a function of the SNR. As expected, all the performance curves are upper and lower bounded by the SE achieved using fully digital beamform-ing approach and hybrid beamforming in [13], respectively. The SE gap between the procedures increases as the value of SNR increases. We observe that the performance of the proposed algorithm is close to the optimal full digital beam-forming scheme. This indicates that the proposed algorithm is a great energy-saving scheme to improve SE performance.

To verify the robustness performance of the proposed solu-tion, we further consider an RIS-assisted system by changing the multiplexing settings (e.g., the number of RIS elements, and data streams). Particularly, In Fig. 2(b), we examine the impact of the EH threshold on the total transmit power constraint. We notice that the performance gains are more prominent from more stringent EH thresholds. Meanwhile, it is observed that when the EH threshold of user is the same, the total transmit power can be improved by increasing the number of RIS elements. Finally, the effect of the number of data streams on the performance of the proposed algorithm is verified in Fig. 2(c). It is clear that the SE of the proposed system increases with the number of data streams when phase shifts with the same resolution are used.

V. CONCLUSION

This letter studies the hybrid beamforming design for RIS-assisted multiuser SWIPT communication. The sum rate maximization problem was formulated subject to the total transmit power and the minimum EH requirement per energy user. To tackle this intractable problem, an iterative algorithm with MMSE and the greedy selection is developed to derive the sub-optimal solution. Numerical simulation verify the effec-tiveness and robustness of the proposed algorithm, in which the proposed hybrid beamforming with RIS can enhance the sum rate performance of SWIPT systems.

REFERENCES

[1] L. R. Varshney, "Transporting information and energy simultaneously," in *Proc. IEEE Int. Symp. Inf. Theory*, 2008, pp. 1612–1616.
[2] X. Zhou, R. Zhang, and C. K. Ho, "Wireless information and power transfer: Architecture design and rate-energy tradeoff," *IEEE Trans. Commun.*, vol. 61, no. 11, pp. 4754–4767, Nov. 2013.
[3] W. Lu et al., "SWIPT cooperative spectrum sharing for 6G-enabled cognitive IoT network," *IEEE Internet Things J.*, vol. 8, no. 20, pp. 15070–15080, Oct. 2021.
[4] S. Gong, Z. Yang, C. Xing, J. An, and L. Hanzo, "Beamforming optimization for intelligent reflecting surface-aided SWIPT IoT networks relying on discrete phase shifts," *IEEE Internet Things J.*, vol. 8, no. 10, pp. 8585–8602, May 2021.
[5] C. Pan et al., "Intelligent reflecting surface aided MIMO broadcasting for simultaneous wireless information and power transfer," *IEEE J. Sel. Areas Commun.*, vol. 38, no. 8, pp. 1719–1734, Aug. 2020.
[6] J. Zhang, G. Zheng, I. Krikidis, and R. Zhang, "Specific absorption rate-aware Beamforming in MISO downlink SWIPT systems," *IEEE Trans. Commun.*, vol. 68, no. 2, pp. 1312–1326, Feb. 2020.
[7] A. Li and C. Masouros, "Energy-efficient SWIPT: From fully digital to hybrid analogcdigital beamforming," *IEEE Trans. Veh. Technol.*, vol. 67, no. 4, pp. 3390–3405, Apr. 2018.
[8] C. Huang et al., "Holographic MIMO surfaces for 6G wireless networks: Opportunities, challenges, and trends," *IEEE Wireless Commun.*, vol. 27, no. 5, pp. 118–125, Oct. 2020.
[9] L. Wei, C. Huang, G. C. Alexandropoulos, C. Yuen, Z. Zhang, and M. Debbah, "Channel estimation for RIS-empowered multi-user MISO wireless communications," *IEEE Trans. Commun.*, vol. 69, no. 6, pp. 4144–4157, Jun. 2021.
[10] O. E. Ayach, R. W. Heath, S. Abu-Surra, S. Rajagopal, and Z. Pi, "The capacity optimality of beam steering in large millimeter wave MIMO systems," in *Proc. IEEE 13th Int. Workshop Signal Process. Adv. Wireless Commun. (SPAWC)*, 2012, pp. 100–104.
[11] C. T. K. Ng and H. Huang, "Linear precoding in cooperative MIMO cellular networks with limited coordination clusters," *IEEE J. Sel. Areas Commun.*, vol. 28, no. 9, pp. 1446–1454, Dec. 2010.
[12] C. Zeng, J.-B. Wang, C. Ding, H. Zhang, M. Lin, and J. Cheng, "Joint optimization of trajectory and communication resource allo-cation for unmanned surface vehicle enabled maritime wireless networks," *IEEE Trans. Commun.*, vol. 69, no. 12, pp. 8100–8115, Dec. 2021.
[13] Z. Chen, N. Zhao, D. K. C. So, J. Tang, X. Y. Zhang, and K.-K. Wong, "Joint altitude and hybrid beamspace precoding optimization for UAV-enabled multiuser mmWave MIMO system," *IEEE Trans. Veh. Technol.*, vol. 71, no. 2, pp. 1713–1725, Feb. 2022.
[14] Z. Yang and Y. Zhang, "Optimal SWIPT in RIS-aided MIMO networks," *IEEE Access*, vol. 9, pp. 112552–112560, 2021.
[15] Y. Ye, L. Shi, X. Chu, and G. Lu, "Throughput fairness guarantee in wireless powered backscatter communications with HTT," *IEEE Wireless Commun. Lett.*, vol. 10, no. 3, pp. 449–453, Mar. 2021.